Analysis of Phosphorylation-dependent Protein Interactions of Adhesion and Degranulation Promoting Adaptor Protein (ADAP) Reveals Novel Interaction Partners Required for Chemokine-directed T cell Migration*[S]

Benno Kuropka‡§ §§, Amelie Witte¶§§, Jana Sticht‡, Natalie Waldt¶, Paul Majkut§‖, Christian P. R. Hackenberger§, Burkhart Schraven¶, Eberhard Krause§‡‡, Stefanie Kliche¶‡‡, and Christian Freund‡ ‡‡**

Stimulation of T cells leads to distinct changes of their adhesive and migratory properties. Signal propagation from activated receptors to integrins depends on scaffolding proteins such as the adhesion and degranulation promoting adaptor protein (ADAP)[1]. Here we have comprehensively investigated the phosphotyrosine interactome of ADAP in T cells and define known and novel interaction partners of functional relevance. While most phosphosites reside in unstructured regions of the protein, thereby defining classical SH2 domain interaction sites for master regulators of T cell signaling such as SLP76, Fyn-kinase, and NCK, other binding events depend on structural context. Interaction proteomics using different ADAP constructs comprising most of the known phosphotyrosine motifs as well as the structured domains confirm that a distinct set of proteins is attracted by pY571 of ADAP, including the ζ-chain-associated protein kinase of 70 kDa (ZAP70). The interaction of ADAP and ZAP70 is inducible upon stimulation either of the T cell receptor (TCR) or by chemokine. NMR spectroscopy reveals that the N-terminal SH2 domains within a ZAP70-tandem-SH2 construct is the major site of interaction with phosphorylated ADAP-hSH3^N and microscale thermophoresis (MST) indicates an intermediate binding affinity (K_d = 2.3 μM). Interestingly, although T cell receptor dependent events such as T cell/antigen presenting cell (APC) conjugate formation and adhesion are not affected by mutation of Y571, migration of T cells along a chemokine gradient is compromised. Thus, although most phospho-sites in ADAP are linked to T cell receptor related functions we have identified a unique phosphotyrosine that is solely required for chemokine induced T cell behavior. ***Molecular & Cellular Proteomics 14: 10.1074/mcp.M115.048249, 2961–2972, 2015.***

From the ‡Freie Universität Berlin, Institut für Chemie und Biochemie, Protein Biochemistry group, Thielallee 63, 14195 Berlin, Germany; §Leibniz-Institut für Molekulare Pharmakologie, Robert-Rössle-Strasse 10, 13125 Berlin, Germany; ¶Otto-von-Guericke-University, Institute of Molecular and Clinical Immunology, Leipziger Strasse 44, 39120 Magdeburg, Germany; ‖RiNA GmbH, Volmerstrasse 9, 12489 Berlin, Germany; **Helmholtz Center for Infection Research (HZI), Department of Immune Control, Inhoffenstrasse 7, 38124 Braunschweig, Germany

Received January 19, 2015, and in revised form, July 29, 2015
Published, MCP Papers in Press, August 5, 2015, DOI 10.1074/mcp.M115.048249

Author contributions: Experiments were conceived by CF, SK, EK and BS and carried out by BK (mass spectrometry, biochemistry), JS & CF (NMR), AW, NW, SK (cell experiments), PM and CPH (synthesis of SNAP-hSH3^N). Data were analyzed by all contributing authors while BK, SK, EK and CF wrote the paper.

[1] The abbreviations used are: ADAP, adhesion and degranulation promoting adaptor protein; APC, antigen presenting cell; CRKL, CRK-like protein; EVL, Ena/VASP-like protein; hSH3, helical extended SH3; hSH3^N, N-terminal hSH3; ICAM, intercellular cell adhesion molecule; ITAM, immunoreceptor-tyrosine-based activation motif; Kd, equilibrium dissociation constant; LAT, linker for activation of T cells; Lck, lymphocyte-specific protein tyrosine kinase; LFA-1, lymphocyte function-associated antigen 1; MST, microscale thermophoresis; PRS, proline-rich sequence; SH2, Src-homology 2; SH3, Src-homology 3; SHIP, SH2-containing inositol phosphatase; SILAC, stable isotope labeling by amino acids in cell culture; SKAP55, Src-kinase associated phosphoprotein of 55 kDa; SLP76, SH2 domain-containing leukocyte protein of 76 kDa; TCR, T cell receptor; MHC, major histocompatibility complex; VCAM, vascular cell adhesion molecule; VLA-4, very late antigen 4; ZAP70, zeta-chain-associated protein kinase of 70 kDa.

T cell migration and the establishment of productive T cell/APC interactions are regulated by the activity of integrins. In resting T cells, integrins are expressed in an inactive state that adopts a conformation with low affinity for their ligands. Members of the intercellular adhesion molecule family (ICAM 1–5) are the physiological ligands of lymphocyte function-associated antigen 1 (LFA-1, αLβ2-integrin) whereas vascular cell adhesion molecule (VCAM) and fibronectin are the ligands for the β1-integrin very late antigen 4 (VLA-4) (1, 2). Triggering of the T cell receptor (TCR) by peptide-major histocompati-

bility complex (MHC) or stimulation of chemokine receptors (*e.g.* CCR7 with CCL21 or CXCR4 with CXCL12) induces a conformational change of the integrins that increases their ligand binding (affinity regulation) and subsequently mediates clustering of integrins at the cell surface (avidity regulation). The intracellular events leading to integrin activation have collectively been termed inside-out signaling. Conversely, ligand-bound integrins transmit a signal to the T cell and thereby promote adhesion, activation, proliferation, and migration of T cells (outside-in signaling) (1, 2).

In both inside-out and outside-in signaling pathways tyrosine phosphorylation of adaptor proteins, either present as transmembrane scaffolds or as transiently membrane-anchored proteins, is a crucial primary event in signal transmission to integrins.

An essential functional module operating at the integrin-membrane-cytoskeleton interface contains the cytosolic adaptor protein ADAP at its core. Ablation of ADAP in mice leads to dysfunctional integrin clustering and activity, thus compromising the adhesive and migratory properties of these cells. In addition to its instantaneous effects on cellular motility, ADAP was shown to act as a regulator of NFκB p65 nuclear translocation (3), a function that might well contribute to the observed modulation of cytokine production, like interleukin-2 (4, 5). A contribution of ADAP to mast cell degranulation has been postulated (6), and its complex formation with cytoskeletal regulators during early phases of phagocytosis in macrophages has been recognized early on (7). ADAP is also critical for normal platelet adhesion (8) and mutations in the human protein have recently been suggested to form an underlying genetic cause for autosomal recessive thrombocytopenia (9).

ADAP interacts with several effectors of T cell function, either constitutively or phosphorylation-dependent. The SH3 domain of SKAP55 (Src-kinase associated phosphoprotein of 55 kDa) interacts with a proline-rich sequence (PRS) stretch in ADAP (Fig. 1*A*) (10, 11), whereas another PRS (FPPPP) is responsible for the interaction with the actin regulator Ena/VASP-like protein (EVL) (12). Membrane binding of the ADAP-SKAP55 complex is conferred by the PH domain of SKAP55 and to a lower extend by the C-terminal hSH3 domain ($hSH3^C$) of ADAP (13–16). Moreover, ADAP is strongly tyrosine-phosphorylated upon TCR stimulation and thereby serves as a hub for SH2 domain-containing proteins such as SLP76, FYN and NCK (Fig. 1*A*) (17–21). Beside these well characterized interactions, several other SH2-domain containing binders were identified by pull-down approaches using phosphorylated peptide baits (Fig. 1*A*) (22, 23). Most of the so far characterized SH2-pTyr interactions in ADAP are mapped to unstructured regions. An exception is Y571, which is located in close proximity to the folded $hSH3^N$ domain of ADAP. Phosphoproteomic profiling of activated T cells has identified Y571 as a major phosphorylation site in ADAP (18, 24–30). Our rationale for the experimental approach chosen here was that the constraints imposed by the folding of the hSH3 domains impact the choice of SH2 domains that bind to such motifs in ADAP.

To meet this challenge, we employed interaction proteomics and immunoprecipitation experiments using different constructs of ADAP that comprise the major phosphotyrosine sites including the two folded hSH3 domains. In particular, Y571, a residue residing at the domain border of the $hSH3^N$ domain, is shown to interact with proteins that are not identified by the peptide pull-down approach. We identify the ZAP70 kinase as the most robust binding partner of pY571 and show that this interaction is maintained in primary T cells. Using NMR spectroscopy we further show that the N-terminal SH2 domain of ZAP70 is responsible for binding and we confirm the direct interaction between the two proteins to be inducible upon T cell receptor or CXCR4 stimulation. Abolishing the interaction by using a Y571F mutation compromises T cell migration along a CXCL12 gradient but does not affect TCR- and CXCR4-mediated adhesion and T cell interaction with APCs. In this way, the Y571F mutant of ADAP provides the striking example of a molecular switch that selectively invokes the migratory, but not the adhesive, signaling pathways in T cells.

EXPERIMENTAL PROCEDURES

Experimental Procedures Available Online—These include experimental constructs; protein expression and purification; synthesis of SNAP-$hSH3^N$; construction of the suppression/re-expression vector of ADAP mutant.

SILAC Cell Culture—Stable isotope labeling by amino acids in cell culture (SILAC) was performed as described (31). RPMI1640 medium deficient in arginine and lysine supplemented with 10% dialyzed FBS was used (SILAC quantification kit, Pierce). The "light" cell population was supplemented with 0.1 g/L L-Lys and 0.2 g/L L-Arg and the "heavy" cell population was supplemented with 0.1 g/L $^{13}C_6$-L-Lys and 0.2 g/L $^{13}C_6$,$^{15}N_4$-L-Arg (Cambridge Isotope Laboratories, Andover, MA). Cells were cultured in heavy or light media for at least five population doublings. Labeling efficiencies were determined by mass spectrometry of tryptic digests of selected SDS-PAGE bands and were found to be >95%.

In Vitro Phosphorylation of Full-length ADAP, GST-$ADAP^{486-783}$, and GST-$hSH3^N$—For pull-down experiments GST-$ADAP^{486-783}$ and GST-$hSH3^N$ (10 μM) were phosphorylated by incubation with the Src kinase Fyn (0.2 μM) in 50 mM Tris-HCl (pH 7.5), 10 mM $MgCl_2$, 0.5 mM EGTA, 0.1 mM Na_3VO_4, 150 mM NaCl, 2 mM DTT, and 2 mM ATP at room temperature for 5 days. For the control experiment no ATP was added. Tyrosine phosphorylation was detected by Western blotting with an anti-phosphotyrosine antibody as described elsewhere (18). Phosphorylation degrees were detected by mass spectrometry after SDS-PAGE and tryptic in-gel digestion as described further below.

For a comprehensive investigation of ADAP phosphorylation sites full-length ADAP (10 μM) was used as substrate for *in vitro* phosphorylation by Fyn (0,8 μM) as described above. Samples obtained at distinct incubation times were collected and directly boiled in SDS sample buffer. After separation by SDS-PAGE ADAP bands were excised and each band was divided for subsequent digestion by trypsin and elastase as described further below.

Pull-down Experiments—For pull-down experiments GST-$ADAP^{486-783}$ (nonphosphorylated and phosphorylated) and GST-$hSH3^N$ (nonphosphorylated and Y571-phosphorylated) were loaded

on 25 μl of glutathione Sepharose 4B beads (GE Healthcare) using 5 mg protein/ml of matrix for 2 h at 4 °C. To obtain cellular lysates, cells were treated with lysis buffer (10 mM Hepes (pH 7.5), 150 mM NaCl, 10 mM $MgCl_2$, 10 mM KCl, 0.5 mM EGTA) with 1% (v/v) Nonidet P-40, 1 mM Na_3VO_4, 3 U/ml Benzonase Nuclease (Sigma, Taufkirchen, Germany), protease inhibitor cocktail (complete, EDTA free, Roche Applied Science) on ice for 30 min, and cell debris were removed by centrifugation for 20 min at 16,000 g at 4 °C. For the pull-down experiment under oxidizing conditions 50 μM H_2O_2 was added to the lysis buffer. Beads were washed four times with ice-cold PBS (including 2 mM H_2O_2 for the experiment under oxidizing conditions) and incubated with 150 μl cell lysate (2×10^7 cells) overnight at 4 °C. Subsequently, the beads were washed four times with ice-cold PBS, and proteins were eluted from the matrix with SDS sample buffer 5 min at 95 °C. Eluates (heavy and light) from pull-downs using SILAC-labeled Jurkat T cell lysates were combined before separation by SDS-PAGE (Tris-glycine gradient gel, 4–20%, Invitrogen). Eluates from pull-downs using primary human T cell lysate ($^{16}O/^{18}O$-labeling) were separated side-by-side.

Sample Preparation and Liquid Chromatography-Tandem Mass Spectrometry—For pull-down experiments using SILAC, Coomassie-stained lanes were cut into 30–40 slices and proteins were digested with trypsin. Gel slices were washed with 50% (v/v) acetonitrile in 50 mM ammonium bicarbonate, shrunk by dehydration in acetonitrile, and dried in a vacuum centrifuge. The dried gel pieces were incubated with 50 ng trypsin (Promega, Madison, WI) in 10 μl of 50 mM ammonium bicarbonate at 37 °C overnight. For identification of phosphorylation sites in full-length ADAP the dried gel pieces were also incubated with 100 ng elastase (Sigma) in 10 μl of 50 mM ammonium bicarbonate at 37 °C overnight. To extract the peptides, 10 μl of 0.5% (v/v) trifluoroacetic acid in acetonitrile was added and the separated liquid was dried under vacuum. For pull-downs using $^{16}O/^{18}O$-labeling, gel lanes corresponding to eluates from GST-$hSH3^N$ and Y571-phosphorylated GST-$hSH3^N$ were cut into 20 slices in a parallel fashion. Tryptic in-gel digestion and $^{16}O/^{18}O$-labeling was performed as described (22). Both pull-down experiments (SILAC and $^{16}O/^{18}O$-labeling) were performed at least twice with switched isotopic labeling (forward and reverse experiments).

For MS analysis, the samples were reconstituted in 6 μl of 0.1% (v/v) TFA, 5% (v/v) acetonitrile in water. Peptides were analyzed by a reversed-phase capillary liquid μM chromatography system (Eksigent NanoLC Ultra, Axel Semrau, Sprockhoevel, Germany) connected to an LTQ Orbitrap XL mass spectrometer (Thermo Scientific). LC separations were performed on a capillary column (PepMap100, C18, 3 μm, 100 Å, 250 mm × 75 μm i.d., Thermo Scientific) at an eluent flow rate of 200 nL/min using a linear gradient of 3–25% B in 75 min with further increase to 50% B. Mobile phase A contained 0.1% formic acid in water, and mobile phase B contained 0.1% formic acid in acetonitrile. Mass spectra were acquired in a data-dependent mode with one MS survey scan (with a resolution of 30,000) in the Orbitrap and MS/MS scans of the four most intense precursor ions in the linear trap quadrupole.

Data Processing and Protein Quantification of Mass Spectrometric Results—For SILAC pull-down experiments, identification and quantification of proteins were carried out with version 1.4.1.2 of the MaxQuant software package as described (32). Data were searched against the human subset of the UniProt protein database (release 12-Dez-2013; 88,479 entries). A maximum of two missed cleavages was allowed. For precursor ions individual mass tolerances were used according to the MaxQuant Software. The mass tolerance of sequence ions was set at 0.35 Da. Methionine oxidation, acetylation of protein N terminus and the acrylamide modification of cysteine were used as variable modifications. False discovery rates were set to 1% based on matches to reversed sequences in the concentrated target-decoy database. All proteins were identified using at least 2 razor/unique and 1 unique peptide (MaxQuant). Protein ratios (MaxQuant normalization) were considered if at least three peptide ratios were quantified in both forward and reverse experiments. A protein was highlighted as a potential phosphorylation-dependent binding partner if its isotope ratios in both forward and reverse experiments were clearly separated from the background binders as defined visually. Depending on the ratio distribution of the particular experiment an individual threshold was used for each experiment. For the baits $ADAP^{486-783}$ and ADAP-$hSH3^N$ (oxidizing conditions) a ratio of >3 and >2 was set for forward and reverse experiments, respectively. In all the other experiments a minimum ratio of 4 was used. In addition, mass spectra of peptides used for quantification of binding proteins were verified manually.

For $^{16}O/^{18}O$-labeled pull-down experiments, Mascot Distiller (version 2.4.3.3) and Mascot Server (version 2.2, Matrix Science, London, UK) were used to search against the human subset of the UniProt protein database (release 12-Dez-2013; 88,479 entries). The mass tolerance of precursor and sequence ions was set to 15 ppm and 0.35 Da, respectively. Relative quantification of proteins was based on $^{18}O/^{16}O$ isotope intensity ratios determined by the Mascot Distiller Quantitation Toolbox. Peptides were used for quantification if their Mascot score was greater than the homology threshold. False discovery rates were estimated to be $<1\%$ based on matches to reversed sequences in the concatenated target-decoy database. The protein ratios were calculated as intensity weighted mean of at least three peptide ratios. Normalization of protein ratios was done manually by dividing them by the mean of all protein ratios.

To identify phosphorylated peptides, probability-based scoring (MASCOT score) was used. In addition, tandem mass spectra of phosphopeptides were manually verified and compared with the theoretical fragment ion spectra. Phosphorylation degrees for each tyrosine residue were calculated by manually comparing relative MS peak intensities of the corresponding peptide/phosphopeptide pairs as described (33, 34). All peptides generated by trypsin and/or elastase digestion with intensities $>10^7$ and all observable charge states were included for relative quantification.

NMR Spectroscopy—NMR spectra were acquired at a Bruker AV700 MHz Avance spectrometer equipped with a triple-resonance cryoprobe. ^1H-^{15}N HSQC spectra of ^{15}N-labeled $hSH3^N$ or ZAP70-tSH2 were acquired at 298K using 175 μM nonphosphorylated ^{15}N-$hSH3^N$ or 60 μM phosphorylated ^{15}N-$hSH3^N$ alone or in the presence of roughly equimolar amounts of ZAP70-tSH2 and 100 μM ^{15}N-ZAP70-tSH2 alone or in the presence of roughly equimolar amounts of (un)phosphorylated $hSH3^N$. All measurements were done in 100 mM NaH_2PO_4 (pH 6.8), 50 mM NaCl, 5 mM DTT with 10% D_2O. Spectra were processed with the Topspin software package (Bruker) and analyzed with CcpNmr Analysis (35). Published $hSH3^N$ assignments (BMRB6536,(36)) were used and assignments for ZAP70-tSH2 were kindly provided by Rutger Folmer as published (37) and—if unambiguously possible—transferred to our spectra. Chemical shift differences were calculated using the formula $\Delta\delta = (\delta H^2 + (0.15 \times \delta N)^2)^{0,5}$ and were defined as significant if higher than the mean value plus the standard deviation.

Synthesis of Phosphorylated Snap-$hSH3^N$—Generation of Snap-$hSH3^N$ is described in the supplemental methods. For *in vitro* phosphorylation, the protein was supplemented with 0.5 mM Na_3VO_4 and 2 mM DTT and Fyn kinase was added at a molar ratio of 1:12. The phosphorylation was started by addition of ATP to a final concentration of 2 mM, whereas the reaction mix lacking ATP served as the nonphosphorylated control. Incubation was at room temperature for 5 days. After determining the phosphorylation degree of Y571 by nanoLC-MS (see above), the Snap-$hSH3^N$ fusion protein was directly used for MST analysis.

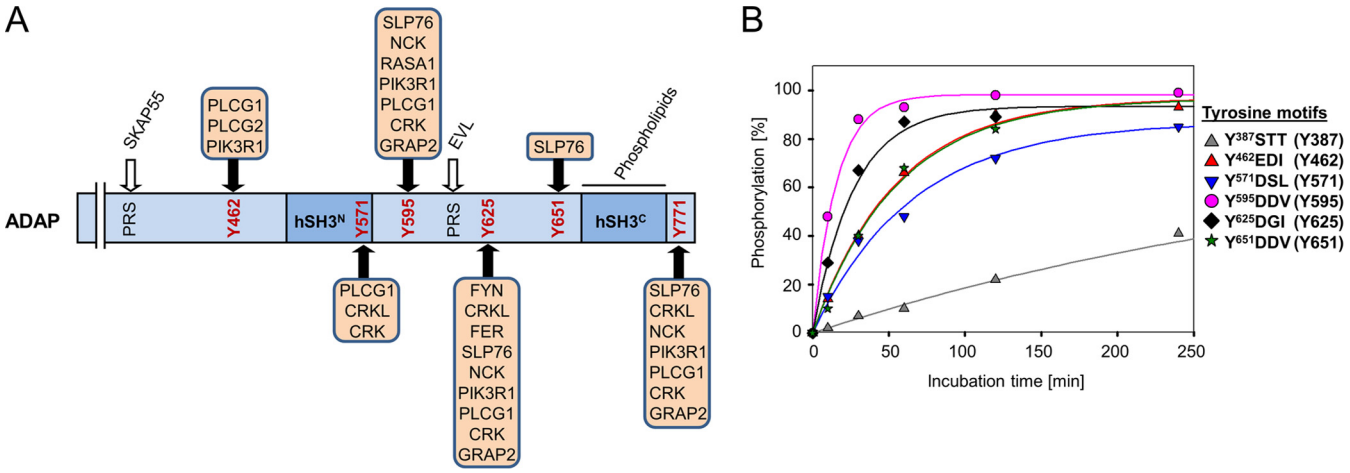

FIG. 1. **Phosphotyrosine sites of ADAP and interaction partners.** *A*, Schematic overview of the ADAP primary structure indicating interaction partners of different phosphotyrosine sites identified by peptide pull-down approaches (22, 23). Black arrows show SH2-pTyr interaction sites. White arrows show interactions dependent on proline rich sequences (PRS). *B*, Fyn kinase catalyzed *in vitro* phosphorylation of full-length ADAP. Identification and relative quantification of phosphorylation degrees of individual tyrosine residues was obtained by mass spectrometry. Phosphorylation degrees were estimated by comparing relative MS peak intensities of the corresponding peptide/phosphopeptide pairs as described (33, 34).

MST Measurements—For MST measurements purified ZAP70-tSH2 was serially diluted over three orders of magnitude in 1x PBS supplemented with 1.75% (v/v) *E. coli* extract of the Easy Xpress Mini Kit as a blocking agent and 0.05% Tween-20 in 200 μl PCR-tubes. Afterward, Snap-hSH3^N was added from a diluted sample in the same buffer to a final concentration of 25 nM, and the samples were gently mixed. The samples were allowed to incubate at room temperature for 5 min before being loaded into standard-treated Monolith^{TM} capillaries (NanoTemper). After placing into the instrument (Monolith NT.115, NanoTemper), the samples were measured by standard protocols at 20% MST power. The changes of the fluorescent thermophoresis signals were plotted against the concentration of the serially diluted ZAP70-tSH2. K_d values were determined using the NanoTemper analysis software (NT Analysis 1.5.37) by fitting the data representing the mean ± S.D. from three independent experiments according to the law of mass action.

Primary Cells, Cell Culture, and Transfection—Primary human T cells were isolated from healthy donors by standard separation methods using AutoMACS (Miltenyi Biotech, Bergisch Gladbach, Germany) maintained in RPMI 1640 medium containing 10% fetal calf serum (FCS; PAN), stable L-glutamine and 2 μg/ml Ciprofloxacin. Approval for these studies was obtained from the Ethics Committee of the Medical Faculty at the Otto-von-Guericke University, Magdeburg, Germany. Informed consent was obtained in accordance with the Declaration of Helsinki. The Jurkat T cell line (JE6.1; ATCC) and the B-cell line (Raji; ATCC) were cultured as previously described (38). Transient transfections of Jurkat T cells were performed as previously described (11) and cultured for 48 h before use.

Adhesion Assay, Conjugate Formation, and Migration—Transfected Jurkat T cells with the indicated suppression/re-expression vectors were used to address TCR/CXCR4-mediated adhesion, conjugate formation and migration after 48 h as previously described (38, 39).

Flow Cytometry—To analyze the cell surface expression of CD18 (MEM48; both provided by V. Horejsi), CD29 (MEM101A; provided by V. Horejsi**),** CD184 (CXCR4; clone 12G5; BD Biosciences) and CD3 (OKT3), cells were stained with the indicated antibodies in combination with APC-conjugated goat anti-mouse/rat IgG (Dianova, Hamburg, Germany) and analyzed using a FACSCalibur flow cytometer and CellQuestPro software (BD Biosciences).

Immunoprecipitation and Western Blot Analysis—Jurkat T cells were left untreated or stimulated for various time points with anti-CD3 antibodies (OKT3 10 μg/ml) or CXCL12 (100 ng/ml) and lysed as previously described (11, 38, 39). Equivalent amounts of protein (determined by Bradford assay (Roth)) were used in precipitation studies (500 μg of total protein from Jurkat T cells). Cell lysates (50 μg of total protein) or immune complexes were separated by SDS-PAGE and transferred to nitrocellulose membranes. Western blots were conducted with the indicated antibodies and developed with the appropriate horseradish peroxidase-conjugated secondary antibodies (Dianova) and the Luminol detection system (Roth). The anti-human ZAP70 rabbit serum (Cell signaling, Danver, MA), anti-Flag M2 mAb and anti-Flag rabbit antibody (Sigma) were used for immunoprecipitation studies. For Western blot analysis the following antibodies were used: anti-Flag M2 mAb, anti-SKAP55 rat mAb (11), anti-phopsho-Y571-ADAP rabbit antibody (generated and purified by Biogenes using the peptide CAVEID-pY-DSLKLKKD), anti-ADAP mAb (BD Biosciences), anti-ZAP70 mAb (BD Biosciences, Dallas, TX), anti-β-actin mAb (Sigma), anti-PLCγ1 mAb (Santa Cruz, Dallas, Texas), pERK1/2 rabbit antibody (Cell signaling), and anti-LAT mAb (eBioscience, San Diego, CA).

Statistical Analysis—Statistical differences were analyzed using Student's *t* test. A $p \leq 0.05$ was considered statistically significant.

RESULTS

The Phosphotyrosine Proteome of ADAP—Interactome analysis of ADAP previously investigated by peptide pull-down approaches (22, 23) (summarized in Fig. 1*A*) revealed a redundant set of SH2 domain containing proteins to bind to different phosphotyrosine sites. All of these proteins belong to signaling networks that are engaged upon T cell receptor stimulation, such as the PI3 kinase pathway, actin reorganization or integrin activation (Fig. 1*A*). We investigated phosphorylation of these sites in full-length ADAP *in vitro* by FYN and confirmed a high degree of phosphorylation for most of them after four hours of incubation with the kinase (Fig. 1*B*). This enabled us to experimentally pose the question whether

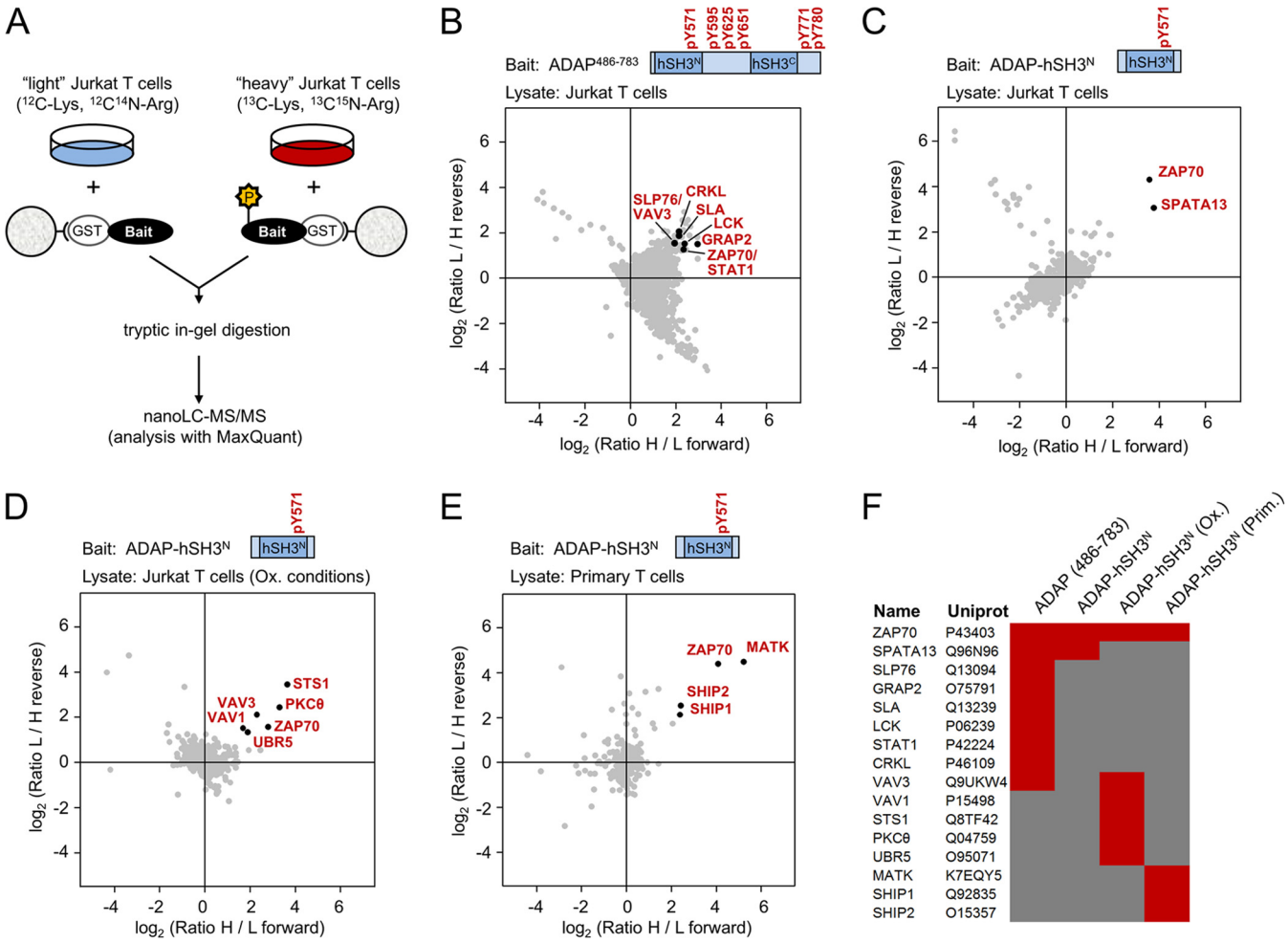

FIG. 2. **Proteomics approach for identification of ADAP binding partners.** *A*, Proteins are metabolically labeled in cell culture using "light" or "heavy" lysine and arginine (SILAC). Phosphorylated and nonphosphorylated bait proteins (GST-ADAP$^{486-783}$ or GST-hSH3^{N}) were incubated with the heavy and light labeled Jurkat T cell lysate, respectively. After combining the samples, proteins were separated by SDS-PAGE. After tryptic in-gel-digestion, peptides were analyzed by nanoLC-MS/MS and proteins were identified and quantified using the MaxQuant software. *B–E*, Scatter plots of heavy/light (forward) and light/heavy (reverse) isotopic ratios of identified proteins from quantitative pull-down experiments using phosphorylated and nonphosphorylated baits. Proteins that showed phosphorylation-dependent enrichment are highlighted. *B*, GST-ADAP$^{486-783}$ incubated with Jurkat T cell lysate. For clarity reasons, only enriched proteins that contain SH2-domains are highlighted. *C*, GST-hSH3^{N} incubated with Jurkat T cell lysate. *D*, GST-hSH3^{N} incubated with Jurkat T cell lysate under oxidizing conditions. *E*, GST-hSH3^{N} incubated with primary human T cell lysate ($^{18}O/^{16}O$ labeling). *F*, Summary of potential phosphorylation-dependent interaction partners identified from pull-down experiments shown in (*B–E*). Enriched proteins are indicated in red whereas gray color indicates no enrichment/identification. Ox. = oxidizing conditions. Prim. = primary human T cell lysates.

a larger sequence context, taking into account the three-dimensional fold of certain regions of the protein, would impose constraints on the interactome that cannot be captured by the reductionist peptide approach. We therefore used a large C-terminal ADAP construct (residues 486–783) comprising most of the known phosphotyrosine motifs and the two structurally characterized hSH3 domains of ADAP for interactome studies. The recombinant GST fusion protein construct was phosphorylated *in vitro* by Fyn kinase and the phosphorylation of individual sites (Y571, Y595, Y625, Y651, Y771 and Y780) was confirmed by mass spectrometry (degree of phosphorylation >70%). Subsequently, the phosphorylated protein was used as bait in the corresponding pull-down experiments of metabolically labeled Jurkat T cell lysates (Fig. 2*A*) whereas nonphosphorylated GST-ADAP$^{486-783}$ served as a control. Pull-down experiments were executed twice with switched isotopic labeling (forward and reverse experiment). The isotope ratio plot shows the relative abundance of all quantified proteins (Fig. 2*B*). A complete list of proteins is shown in supplemental Table S1. Proteins displaying strong isotope enrichment in both experiments are indicative of specific phosphorylation-dependent binding of the protein. In contrast, background proteins that cannot be completely washed from the resin despite repeated washing steps, or proteins binding regardless of the phosphorylation (nonphosphospecific binders) show isotope ratios of about 1. Contam-

inants and the bait protein itself are easily identified in these plots because they are present only in the light form (top left quadrant), whereas differences in the heavy and light cell lysates manifest either in the top left or bottom right quadrant. All proteins with SH2-domains that showed phosphorylation-dependent enrichment to ADAP$^{486-783}$ are indicated in Fig. 2*B*. In part these proteins match with the proteins found in the previous peptide binding experiments (*e.g.* SLP76, GRB2, CRKL), whereas other proteins were not identified before (*e.g.* ZAP70, SLA).

We argued that for the latter proteins structural context is important. Because Y571 is also among the most frequently found phosphotyrosine sites in T cells (40) we decided to individually express the hSH3^{N} domain, and probe its phosphorylation-dependent binding properties. As before, we used *in vitro* phosphorylation by the Fyn kinase to site-specifically modify the stable ADAP-hSH3^{N} construct (ADAP$^{486-579}$). Selective ("preparative") phosphorylation of Y571 was verified by mass spectrometry (supplemental Fig. S1*A*) and is >70% whereas the degree of phosphorylation of other tyrosines in the hSH3^{N} domain was <2% (data not shown). Because Y571 localizes directly at the domain border of the hSH3^{N} domain (14, 15), we used NMR spectroscopy to confirm that phosphorylation of Y571 does not change the global conformation of the protein (supplemental Fig. S1*B*). As for the larger C-terminal construct pull-down experiments with Jurkat T cell lysates were performed and the isotope ratio plots in Fig. 2*C* show the relative abundance of all quantified proteins. Complete lists of proteins are shown in supplemental Table S2. The most consistent and robustly enriched protein binding to the phosphorylated GST-hSH3^{N} was indeed identified as ZAP70, confirming the results obtained with the whole C-terminal fragment of ADAP (Fig. 2*B*). ZAP70 is a tyrosine kinase that is normally associated with the phosphorylated cytoplasmic domains of the TCR zeta-chain (41). The Rac/Cdc42 exchange factor SPATA13 also showed significant enrichment (Fig. 2*C*). Interestingly, peptide pull-down experiments using a short sequence comprising Y571 did not reveal these interactions (Fig. 1*A*), lending support for the hypothesis that the structural context of the hSH3^{N} domain modulates the interaction profile of this very tyrosine. In this regard, we also probed whether oxidizing conditions would further modulate the interaction profile of hSH3^{N}, because an intramolecular disulfide bond can be formed between two cysteines at position 519 and 520 of the domain thereby conceivably changing the potential binding surface surrounding Y571 (42, 43). Confirming, the oxidized hSH3^{N} domain binds ZAP70 also in a phosphorylation-dependent manner (Figs. 2*D*, 2*F*, and supplemental Table S3). However, a set of proteins (STS-1, VAV1, PKCθ, and UBR5) was found to be specifically enriched by phosphorylated and oxidized hSH3^{N} when compared with phosphorylated, reduced hSH3^{N}. Interestingly, STS-1 is postulated to inhibit T cell signaling via binding and potentially dephosphorylating ZAP70 (44).

The interaction between ADAP and ZAP70 has not been observed before and suggests a direct link between two key players of T cell signal transduction. Therefore we aimed to confirm the interaction in primary cells and used lysate from purified human T cells in combination with $^{18}O/^{16}O$ labeling to confirm the interaction. Indeed, we again characterized ZAP70 as one of the most highly enriched proteins, in addition to the tyrosine kinase MATK and the lipid phosphatases SHIP-1 and SHIP-2 (Figs. 2*E*, 2*F*, and supplemental Table S4). Because SHIP phosphatases are not expressed in Jurkat T cells (45) our findings point toward a potential link between ADAP and PI3-kinase signaling that so far has escaped the attention of T cell pathway analysis. The robustness of ZAP70 identification in all the pull-down experiments is further corroborated by the large number of peptides that were found for this protein. The protein isotope ratios plotted against the number of peptides used for quantification for each pull-down experiment (Fig. 2*B*–2*E*) are indicated in supplemental Fig. S2 with the same proteins highlighted in red.

The SH2 Domains of ZAP70 Interact with a Defined Epitope in ADAP Flanking Y571—The SH2 domains of ZAP70 are essential for its function by acting as docking sites for the ITAMs of the TCR complex. Given the similarity of the sequence Y^{571}DSL of ADAP to individual ITAM tyrosines we argued that the ADAP-ZAP70 interaction is mediated by either of the two SH2 domains of ZAP70. To assess this point, we performed NMR studies. Equimolar amounts of a ZAP70-fragment (ZAP70-tSH2) encompassing the two SH2 domains connected by the 50 amino acid interdomain A linker were added to the ^{15}N-labeled hSH3^{N} domain of ADAP in its non-phosphorylated and phosphorylated form, respectively. Representative regions of NMR HSQC spectra before and after addition of ZAP70 for each form are displayed in Fig. 3*A*, whereas the full spectra are shown in supplemental Fig. S3*A* and S3*B*. Interestingly, addition of ZAP70-tSH2 to the phosphorylated hSH3^{N} domain leads to an average reduction of 50% in signal intensity indicating complex formation. A reduction clearly beyond this overall line-broadening is only observed for resonances in the vicinity (S573, L574, shown in Fig. 3*A*, left panel) or spatial proximity (L515, A516, supplemental Fig. S3A) of phosphorylated Y571. These amino acids are therefore likely to define a contiguous binding epitope highlighted in Fig. 3*B*. In contrast, spectra of ^{15}N-labeled unphosphorylated hSH3^{N} domain of ADAP showed only slight alterations in peak intensity upon addition of ZAP70-tSH2 (Fig. 3*A*, right panel, supplemental Fig. S3*B*).

In the complementary experiment where the phosphorylated hSH3^{N} is added to ^{15}N-labeled ZAP70-tSH2, several resonances also lost intensity. ZAP70-tSH2 residues affected upon binding to hSH3^{N} are located in both SH2 domains, with residues in the N-terminal domain such as R17 and L40 showing the strongest signal reduction (Fig. 3*C*, left panel, supplemental Fig. S3*C*). Both residues are located within the

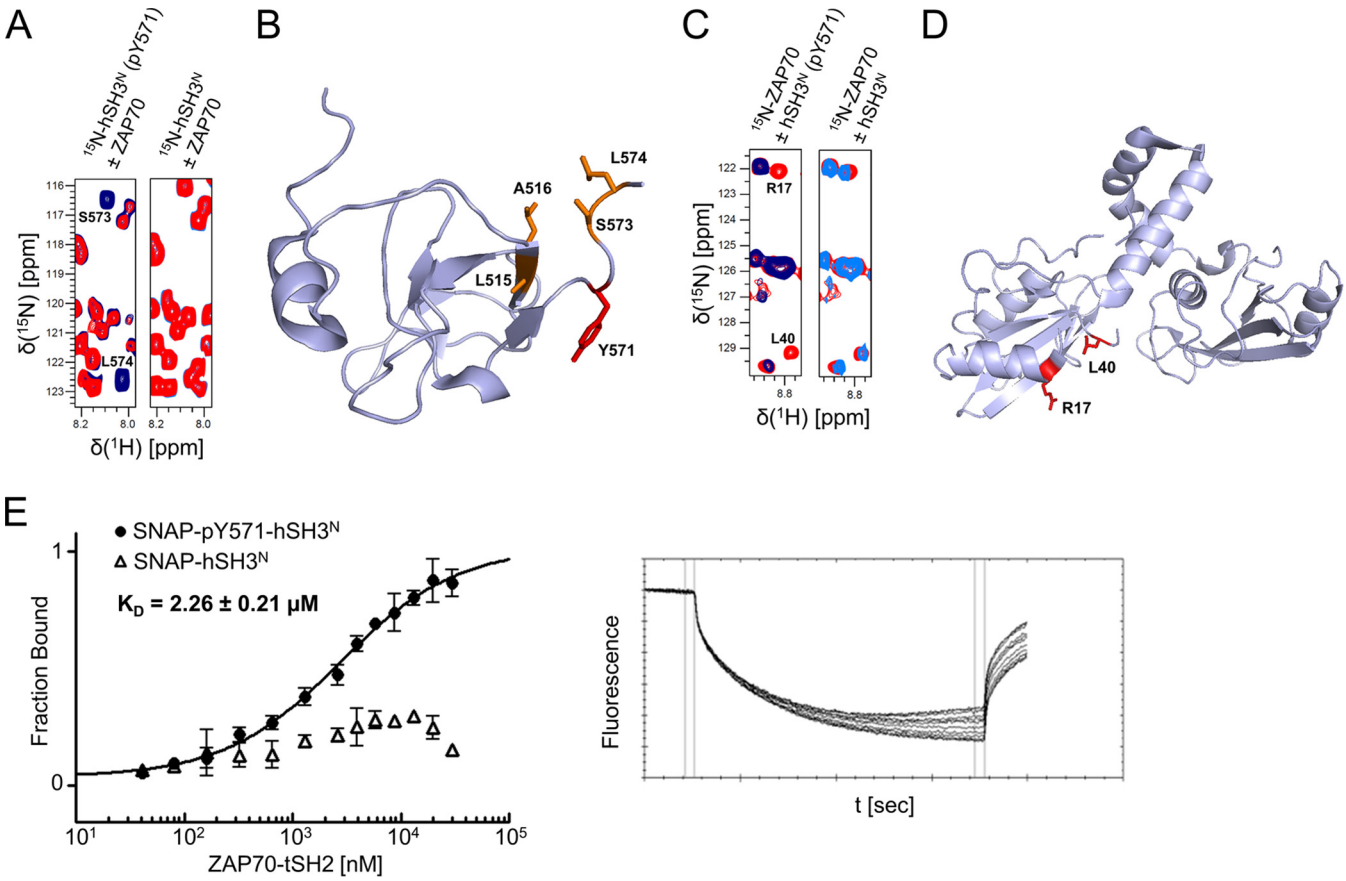

FIG. 3. **Binding studies of the ADAP-ZAP70 interaction.** *A*, Overlay of a region of ^{1}H-^{15}N-HSQC spectra reflecting changes in ^{15}N-labeled hSH3^{N} upon ZAP70 binding. The overlay of phosphorylated hSH3^{N} in the absence (dark blue) and presence (red) of equimolar amounts of ZAP70-tSH2 is shown in the left panel whereas the corresponding control experiment with nonphosphorylated hSH3^{N} is shown on the right (light blue in the absence and red in the presence of ZAP70-tSH2). Resonances of residues displaying significant line broadening are indicated by amino acid type and number. *B*, Three-dimensional structure representation of the hSH3^{N} domain (PDB ID: 2GTJ) indicating the residues that are affected strongly by ZAP70-tSH2 binding. Resonances of phosphorylated hSH3^{N} clearly reduced in intensity upon addition of ZAP70-tSH2 are colored orange (residues L515, A516, S573, L574). Y571 is colored in red. *C*, Superimposed regions of ^{1}H-^{15}N-HSQC spectra reflecting changes in ^{15}N-labeled ZAP70-tSH2 upon hSH3^{N} binding. The overlay of ZAP70-tSH2 is shown for spectra taken in the absence (red) and presence of equimolar amounts of phosphorylated hSH3^{N} (dark blue, left panel) or unphosphorylated hSH3^{N} (light blue, right panel). *D*, Three-dimensional structure representation of ZAP70-tSH2 domain (PDB ID: 1M61) indicating the two residues (R17, L40) that are affected strongly by phosphorylated hSH3^{N} binding. *E*, Microscale thermophoresis data showing the binding of Y571-phosphorylated Snap-hSH3^{N} (25 nM) (solid dots) and the corresponding nonphosphorylated domain (25 nM) (triangles) upon addition of increasing concentrations of ZAP70-tSH2 (41 nM to 44 μM). The affinity (K_d = 2.26 ± 0.21 μM) was determined by fitting the data (representing the mean ± S.D. from three independent experiments) according to the law of mass action. The graph on the right exemplarily shows the thermophoretic running behavior of Y571-phosphorylated Snap-hSH3^{N} upon ZAP70-tSH2 binding at 20% MST power.

N-terminal SH2 domain, as highlighted in Fig. 3*D*. In contrast, the addition of unphosphorylated hSH3^{N} induced only slight changes in signal intensities (Fig. 3*C*, right panel, supplemental Fig. S3*D*). Taken together, these results clearly demonstrate the direct interaction of Y571-phosphorylated hSH3^{N} of ADAP with the ZAP70-tSH2.

For quantitative assessment of the interaction, we determined the equilibrium dissociation constant (K_d) between phosphorylated hSH3^{N} and ZAP70-tSH2 by MST. This method allows the determination of K_d values in solution (46) and was successfully applied for characterization of protein interactions of the phosphorylated linker region of ADAP (ADAP$^{570-690}$) (47). Standard MST requires one partner to be fluorescently labeled. Therefore, the hSH3^{N} domain of ADAP was fused C-terminally to the Snap-tag (48) and expressed *in vitro*. Fluorescence labeling occurs co-translationally whereas phosphorylation is subsequently achieved *in vitro* with Fyn kinase (degree of phosphorylation >70%, as confirmed by MS). MST experiments with increasing concentrations of purified ZAP70-tSH2 (41 nM to 44 μM) clearly affected the thermophoretic motion of phosphorylated hSH3^{N} (Fig. 3*E*, right). Fitting the curves from three independent experiments to a two-state model of binding resulted in a K_d of 2.26 ± 0.21 μM (Fig. 3E, left). In the corresponding control experiment using the nonphosphorylated Snap-hSH3^{N}, no binding to ZAP70-tSH2 was observed.

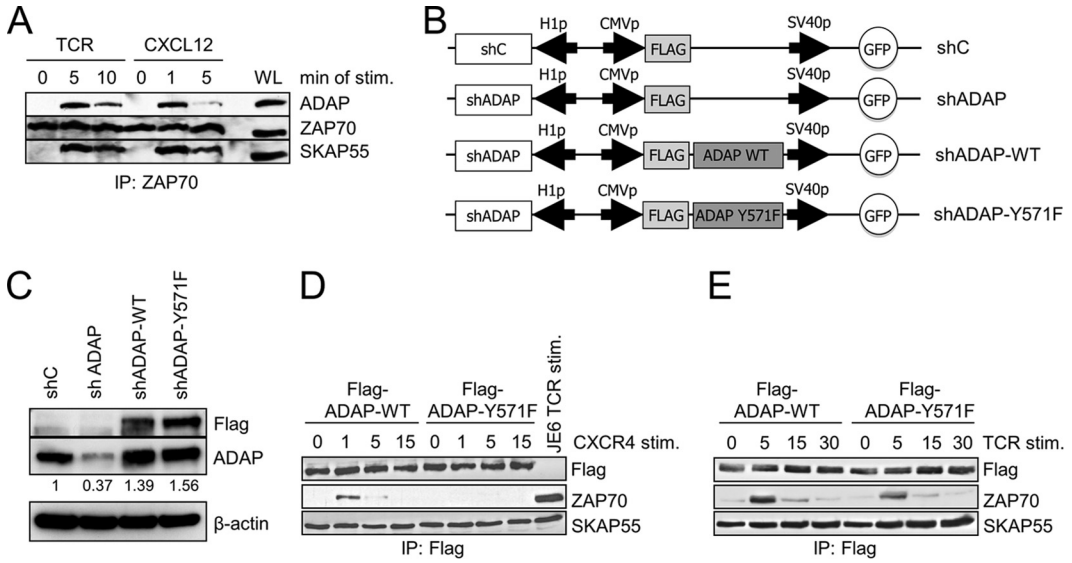

FIG. 4. **Co-immunoprecipitation studies of ADAP and ZAP70.** *A*, Jurkat T cells were either left untreated, stimulated with anti-CD3 antibodies (TCR) or CXCL12 for the indicated time points. Lysates were used for immunoprecipitation using anti-ZAP70 antibody. Precipitates were analyzed by Western blotting with the indicated antibodies. WL denotes whole lysates. *B*, Schematic representation of the suppression/re-expression vectors used in this study. *C*, Jurkat T cells were transfected with suppression/re-expression constructs which do not suppress endogenous ADAP (shC) or reduce the protein level of ADAP (shADAP) and re-express a Flag-tagged shRNA-resistant wild type form of ADAP (shADAP-WT) or its Y571F mutant (shADAP-Y571F). At 48 h post-transfection, whole-cell extracts were harvested, separated by SDS-PAGE, transferred, and blotted for ADAP, Flag, and β-actin (loading control). The suppression of ADAP, re-expressed Flag-tagged WT, and Y571 mutant were quantified using the ImageQuant software to determine the endogenous ADAP band intensity ratio. D, E, Jurkat T cells were transfected as described in (*C*) and stimulated with CXCL12 (*D*) or anti-CD3 antibodies (*E*) for the indicated time points. Lysates were used for immunoprecipitation using an anti-Flag antibody. Precipitates were analyzed by Western blotting using the indicated antibodies. TCR-stimulated Jurkat T cell lysate served as positive control.

The ADAP and ZAP70 Interaction is Inducible in a Cellular Context—To validate the phosphorylation status of ADAP at Y571 we generated a phospho-specific antibody against a peptide containing the phosphorylated tyrosine. With this pY571-specific antibody we observed that phosphorylation of this residue is increased ~2-fold upon TCR or CXCR4 stimulation (supplemental Fig. S4). Subsequently co-immunoprecipitation experiments were performed to validate the interaction between ADAP and ZAP70 *in vivo*. As shown in Fig. 4*A*, TCR stimulation as well as CXCL12 treatment of Jurkat T cells led to an inducible association of ADAP and ZAP70. The functional integrity of ADAP is indicated by coprecipitation of SKAP55, a constitutive binding partner of ADAP (10). To address the question of whether the interaction of ADAP and ZAP70 is mediated by ADAP-Y571, we made use of a suppression/re-expression vector system that allowed shRNA-mediated suppression of endogenous ADAP and simultaneous re-expression of Flag-tagged wildtype (WT) or ADAP-Y571F mutant (Fig. 4*B*). Indeed, although expression of endogenous ADAP was strongly reduced, re-expression of either Flag-WT or mutant Flag-ADAP at nearly endogenous levels was achieved with this system (Fig. 4*C*). We then probed the interaction of the two proteins by immunoprecipitation of Flag-tagged ADAP and found that the binding of ZAP70 to the WT protein is inducible when stimulated by either chemokine (Fig. 4*D*) or TCR (Fig. 4*E*). Interestingly, the time-dependent interaction peaks at 1 min for chemokine and at 5 min for TCR triggering, probably reflecting the different phosphorylation kinetics for Y571 under these two conditions as shown in supplemental Fig. S4. Expression of Flag-tagged ADAP-Y571F mutant did not result in co-precipitation of ZAP70 upon chemokine treatment (Fig. 4*D*), whereas ZAP70 binding to ADAP upon TCR activation was slightly reduced, but not abolished by the mutant (Fig. 4*E*). To verify that under conditions of TCR stimulation the LAT/PLCγ1/SLP76 signalosome serves as a molecular scaffold indirectly linking ADAP to ZAP70 we performed co-immunoprecipitation experiments. Using either Flag-tagged wild type or Y571F mutant of ADAP the presence of ZAP70, LAT, PLCγ1, and SLP76 was verified as previously described for the ZAP70, LAT or SLP76 interactome (supplemental Fig. S5) (49). In contrast to TCR stimulation it was previously shown that this supramolecular assembly is not formed upon chemokine stimulation (39). Thus, the phosphorylation of Y571 of ADAP seems mandatory for the interaction between ADAP and ZAP70 only after CXCR4 stimulation.

Migration but not Adhesion is Dependent on ADAP-Y571 Phosphorylation in T cells—ADAP and ZAP70 have both been found to regulate integrin activation upon TCR and chemokine stimulation to facilitate T cell interactions with APCs or migration along chemokine gradients (39, 50–52). To assess the role of ADAP-Y571 for these cellular processes we again

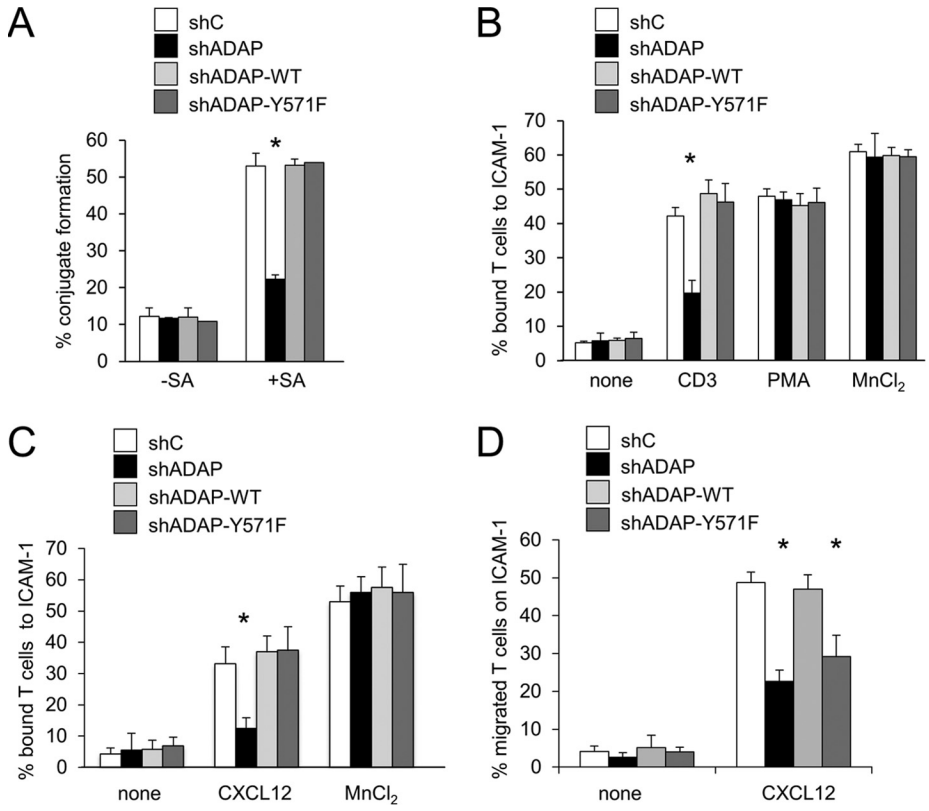

FIG. 5. **The Y571 mutant of ADAP does not affect TCR-mediated adhesion but chemokine-directed T cell migration.** A–D, Jurkat T cells were transfected as described in Fig. 4*B* and 4*C*. *A*, Cells were analyzed for their ability to form conjugates with DDAO-S.E. (red)-stained Raji B cells that were loaded with (+) or without (-) superantigen (SA). The percentage of conjugates was assessed by flow cytometry. *B*, Cells were analyzed for their ability to adhere to ICAM-1-coated wells in a resting state or upon stimulation with anti-CD3 antibody (TCR), phorbol myristate acetate (PMA), or $MnCl_2$. Adherent cells were counted and calculated as percentage of input (2×10^5 cells). *C*, Cells were analyzed for their ability to adhere to ICAM-1-coated wells in a resting state or upon stimulation with CXCL12 or $MnCl_2$. Adherent cells were counted and calculated as a percentage of input (2×10^5 cells). *D*, Cells were placed into the upper part of transwell chambers coated with ICAM-1. Subsequently, cells were incubated in the absence or presence of CXCL12 in the lower chamber for 2 h. Migrated T cells (lower chamber) were counted and calculated as percentage of input cell numbers. Data represent the mean ± S.D. of three independent experiments (*$p \leq 0.05$).

made use of the suppression/re-expression vector system (Fig. 4*B*, 4*C*). We first analyzed cell pair formation between transfected Jurkat T cells and superantigen-loaded Raji B cells, but did not observe an influence of the ADAP-Y571F mutation on conjugate formation (Fig. 5*A*). Next, we stimulated T cells using anti-CD3 antibodies or CXCL12, and then assessed T cell adhesion to ICAM-1 coated plates (Fig. 5*B* and 5*C*, respectively). Notably, T cells expressing the Y571F mutant showed comparable levels of adhesion as cells re-expressing wild type ADAP under both stimulation conditions, whereas a significant reduction of adhesion was observed in the absence of endogenous ADAP, as previously reported (Fig. 5*B*, 5*C*) (5, 39, 51). In accordance with published results, PMA bypassed the requirement for ADAP and Mn^{2+} treatment served as a positive control of the adhesive capacity of these cells. These controls indicate that the activation of LFA-1 following TCR or CXCR4 stimulation is not compromised by the Y571F mutation.

In contrast, significant changes were observed when the migration property of the transfectants was analyzed using a transwell migration assay after CXCL12 stimulation (Fig. 5*D*). Indeed, cells expressing the Y571F mutant of ADAP showed a significant reduction in migration, although the effect was slightly milder compared to the cells treated with anti-shRNA ADAP alone. Of note, the impaired migration was not due to altered expression levels of the TCR, CXCR4, or integrins (supplemental Fig. S6). Thus, although TCR-mediated functions were not compromised by the Y571F mutant, migration of cells along a CXCL12-gradient is significantly affected.

DISCUSSION

Tyrosine phosphorylation is of central importance in T cell activation and the engagement/activation of receptor-proximal tyrosine kinases is an initial event in many signaling pathways. Most phosphotyrosines are contained in short motifs of intrinsically unstructured regions of the corresponding signaling proteins. Specificity for these short motifs is usually limited, leading to promiscuous binding that allows for the dynamic exchange of signaling molecules (53). In contrast, phosphorylation within or in the vicinity of a defined three-

dimensional protein fold harbors the potential that specificity is tuned by a conformational epitope rather than a linear motif. Utilizing a construct of ADAP (ADAP$^{486-783}$) that comprises most phosphotyrosines as well as the two folded hSH3 domains in pull-down experiments, we show that several of the peptide-based assignments of ADAP interaction partners are reproduced. However, other interactions seem to depend on the larger structural context. In particular, the hSH3^{N} domain contains a single highly phosphorylated tyrosine and our results define ZAP70 as the predominant and robust binding partner of this particular phosphosite. Interestingly, ZAP70 was not found to be enriched by mass spectrometry when utilizing a linear motif containing phosphorylated Y571 as bait, indicating that the three-dimensional context (as in hSH3^{N}) and not only the neighboring amino acids (as in the peptide) determine the specificity of phospho-Y571 binding.

In order to be specific, the interaction between ADAP and ZAP70 has to be adequately balanced: To render it inducible and regulated by an upstream tyrosine kinase, the interaction should depend to a large degree on the phosphorylated residue (Y571). To make it specific, regions of the adjacent hSH3^{N} should contribute to binding, or, alternatively, this three-dimensional epitope could "deselect" against the majority of "motif" based interaction partners. For example, because the surface residues of protein domains such as SH2 are less well conserved for regions outside the binding pocket, the ADAP hSH3^{N} domain surface geometry and charge distribution in the vicinity of Y571 might well be incompatible with the defined docking of certain SH2 domain containing proteins. In line with this argument and considering that we use a large excess of bait protein in our domain-based pull-down we do not enrich any of the other SH2 domain containing proteins when compared with previous phosphopeptide enrichments (18, 22).

Phosphorylated Y571 is predominantly recognized by the N-terminal SH2 (N-SH2) domain of ZAP70 and the residues displaying the largest signal reduction in our NMR studies (R17, L40) are identical to those that are line-broadened when ZAP70-tSH2 binds to the singly phosphorylated ITAM peptides pYNEL or pYDVL (37). The core of the ADAP sequence pY^{571}DSL is very similar to a single ITAM motif, and residues R17 and L40 directly interact with the phosphate group of the ligand (54). Thus, we conclude that the N-terminal SH2 domain of ZAP70 is the preferred pY571-accommodating domain. A contribution of hSH3^{N} epitopes other than Y571 are indirectly supported by the finding that the binding affinity of ZAP70-tSH2 and ADAP-Y571 is strong (2 μM) compared with singly phosphorylated ITAMs (143 μM and 333 μM) but weak with respect to the doubly phosphorylated ITAM (32 nM) (55). Thus, under competitive conditions with trace amounts of phosphorylated TCR, phospho-ADAP would be the preferred binding partner for ZAP70, whereas TCR engagement would lead to predominant binding to the ITAM motifs.

Our results show that chemokine stimulation leads to a Y571-dependent association between ADAP and ZAP70. In contrast, upon TCR stimulation, complex formation of ADAP and ZAP70 is not solely dependent on this single tyrosine because a larger TCR-associated complex is maintained in our experiment that contains both molecules (supplemental Fig. S5) (49). An indirect association of ADAP-Y571F with ZAP70 after TCR triggering is also supported by the finding that the other major tyrosine phosphorylation sites of ADAP are not recognized by ZAP70 in pull-down experiments (18, 22, 56). Also, when the TCR is fully phosphorylated in its cytoplasmic domains upon TCR stimulation, it will be the prime target for the tandem SH2 domains of ZAP70, which is, in this way, recruited to the membrane for further activation by Lck. However, after CXCR4 stimulation there is only a weak basal phosphorylation of the TCR complex, and ZAP70 is potentially recruited to different compartments (57); signaling molecules such as ADAP may provide the ITAM-like motifs that capture the ZAP70 SH2 domains under these conditions.

Interestingly, we found the phosphatase STS-1 as a binding partner of ADAP-hSH3^{N} under oxidizing conditions. Because a local increase in reactive oxygen species is thought to accompany T cell stimulation (58), it is well conceivable that STS-1 might be bound directly or indirectly via ZAP70 under oxidizing conditions, thereby modulating the activity of the kinase. Such a regulatory role has been suggested by the use of previous substrate-trapping mutants of STS-1 that identified ZAP70 as a putative target (44).

The identification of an ADAP mutant (Y571F) that selectively affects the migratory behavior of T cells (Fig. 5) is surprising, because depletion of the full-length protein leads to impaired adhesion as well as migration. The latter finding is in line with a large body of evidence that assigns a pivotal function of ADAP to inside-out and outside-in signaling (reviewed in (1, 59)). However, it has remained enigmatic how ADAP confers this dual functionality. Our results now show that tyrosine phosphorylation at a particular site, Y571, is the critical determinant for distinguishing the two pathways. Although several other tyrosines are phosphorylated in ADAP and are bound by effectors of the TCR or integrin inside-out/outside-in signaling pathways (4, 5, 18, 51, 60, 61), it is the Y571 site that confers commitment to migration instead of adhesion. Differential (de-)phosphorylation of this residue is conceivable as the decisive triggering event. However, availability of interacting molecules such as ZAP70 could also be the threshold-defining step, and it is worth noting that phosphorylation of the actin regulatory VAV1 depends on ZAP70, and is prominent after 5 min of CXCL12 stimulation (62). Longer stimulation times (>8 min) also lead to co-localization of CXCR4 and the TCR, thereby allowing CXCR4 to enhance TCR-specific signals (57). Under migratory conditions it is unlikely that such co-segregation of receptors is sustained; one possibility is that ADAP recruitment of ZAP70 prevents the pre-emptive binding of the kinase to small amounts of

phosphorylated TCR. Moreover, because ADAP is directly linked to cytoskeletal dynamics (20), it is conceivable that Y571 phosphorylation is required for linking its scaffolding function at the membrane with actin regulatory events that are critical for maintaining the motility but not the adhesive mode of migrating T cells.

Acknowledgments—We thank Arthur Weiss for providing the ZAP70 constructs. We thank Rutger Folmer for the ZAP70-tSH2 NMR assignments and Michael Schümann for help with the LC-MS/MS experiments. We thank Anke Ramonat and Kathrin Motzny for technical assistance.

* This work was supported by the DFG grants SFB 854 (B12 and B10), SFB958 (A7), SFB765 (B5 and C4), and GRK 1167 (TP11).

[S] This article contains supplemental Figs. S1 to S6 and Tables S1 to S4.

§§ These authors contributed equally.

‡‡ To whom correspondence should be addressed: Freie Universität Berlin, Thielalle 63, Berlin 14195, Germany. Tel.: 030-83851187; E-mails: christian.freund@fu-berlin.de; ekrause@fmp-berlin.de; stefanie.kliche@med.ovgu.de.

REFERENCES

1. Hogg, N., Patzak, I., and Willenbrock, F. (2011) The insider's guide to leukocyte integrin signalling and function. *Nat. Rev. Immunol.* **11,** 416–426
2. Springer, T. A., and Dustin, M. L. (2012) Integrin inside-out signaling and the immunological synapse. *Curr. Opin. Cell Biol.* **24,** 107–115
3. Medeiros, R. B., Burbach, B. J., Mueller, K. L., Srivastava, R., Moon, J. J., Highfill, S., Peterson, E. J., and Shimizu, Y. (2007) Regulation of NF-kappaB activation in T cells via association of the adapter proteins ADAP and CARMA1. *Science* **316,** 754–758
4. Griffiths, E. K., Krawczyk, C., Kong, Y. Y., Raab, M., Hyduk, S. J., Bouchard, D., Chan, V. S., Kozieradzki, I., Oliveira-Dos-Santos, A. J., Wakeham, A., Ohashi, P. S., Cybulsky, M. I., Rudd, C. E., and Penninger, J. M. (2001) Positive regulation of T cell activation and integrin adhesion by the adapter Fyb/Slap. *Science* **293,** 2260–2263
5. Peterson, E. J., Woods, M. L., Dmowski, S. A., Derimanov, G., Jordan, M. S., Wu, J. N., Myung, P. S., Liu, Q. H., Pribila, J. T., Freedman, B. D., Shimizu, Y., and Koretzky, G. A. (2001) Coupling of the TCR to integrin activation by Slap-130/Fyb. *Science* **293,** 2263–2265
6. Geng, L., Pfister, S., Kraeft, S. K., and Rudd, C. E. (2001) Adaptor FYB (Fyn-binding protein) regulates integrin-mediated adhesion and mediator release: differential involvement of the FYB SH3 domain. *Proc. Natl. Acad. Sci. U.S.A.* **98,** 11527–11532
7. Coppolino, M. G., Krause, M., Hagendorff, P., Monner, D. A., Trimble, W., Grinstein, S., Wehland, J., and Sechi, A. S. (2001) Evidence for a molecular complex consisting of Fyb/SLAP, SLP-76, Nck, VASP and WASP that links the actin cytoskeleton to Fcgamma receptor signalling during phagocytosis. *J. Cell Sci.* **114,** 4307–4318
8. Kasirer-Friede, A., Moran, B., Nagrampa-Orje, J., Swanson, K., Ruggeri, Z. M., Schraven, B., Neel, B. G., Koretzky, G., and Shattil, S. J. (2007) ADAP is required for normal alphaIIbbeta3 activation by VWF/GP Ib-IX-V and other agonists. *Blood* **109,** 1018–1025
9. Hamamy, H., Makrythanasis, P., Al-Allawi, N., Muhsin, A. A., and Antonarakis, S. E. (2014) Recessive thrombocytopenia likely due to a homozygous pathogenic variant in the FYB gene: case report. *BMC Med. Gen.* **15,** 135
10. Marie-Cardine, A., Hendricks-Taylor, L. R., Boerth, N. J., Zhao, H., Schraven, B., and Koretzky, G. A. (1998) Molecular interaction between the Fyn-associated protein SKAP55 and the SLP-76-associated phosphoprotein SLAP-130. *J. Biol. Chem.* **273,** 25789–25795
11. Kliche, S., Breitling, D., Togni, M., Pusch, R., Heuer, K., Wang, X., Freund, C., Kasirer-Friede, A., Menasche, G., Koretzky, G. A., and Schraven, B. (2006) The ADAP/SKAP55 signaling module regulates T-cell receptor-mediated integrin activation through plasma membrane targeting of Rap1. *Mol. Cell. Biol.* **26,** 7130–7144
12. Lehmann, R., Meyer, J., Schuemann, M., Krause, E., and Freund, C. (2009) A novel S3S-TAP-tag for the isolation of T-cell interaction partners of adhesion and degranulation promoting adaptor protein. *Proteomics* **9,** 5288–5295
13. Burbach, B. J., Srivastava, R., Ingram, M. A., Mitchell, J. S., and Shimizu, Y. (2011) The pleckstrin homology domain in the SKAP55 adapter protein defines the ability of the adapter protein ADAP to regulate integrin function and NF-kappaB activation. *J. Immunol.* **186,** 6227–6237
14. Heuer, K., Arbuzova, A., Strauss, H., Kofler, M., and Freund, C. (2005) The helically extended SH3 domain of the T cell adaptor protein ADAP is a novel lipid interaction domain. *J. Mol. Biol.* **348,** 1025–1035
15. Heuer, K., Sylvester, M., Kliche, S., Pusch, R., Thiemke, K., Schraven, B., and Freund, C. (2006) Lipid-binding hSH3 domains in immune cell adapter proteins. *J. Mol. Biol.* **361,** 94–104
16. Raab, M., Smith, X., Matthess, Y., Strebhardt, K., and Rudd, C. E. (2011) SKAP1 protein PH domain determines RapL membrane localization and Rap1 protein complex formation for T cell receptor (TCR) activation of LFA-1. *J. Biol. Chem.* **286,** 29663–29670
17. Krause, M., Sechi, A. S., Konradt, M., Monner, D., Gertler, F. B., and Wehland, J. (2000) Fyn-binding protein (Fyb)/SLP-76-associated protein (SLAP), Ena/vasodilator-stimulated phosphoprotein (VASP) proteins and the Arp2/3 complex link T cell receptor (TCR) signaling to the actin cytoskeleton. *J. Cell Biol.* **149,** 181–194
18. Sylvester, M., Kliche, S., Lange, S., Geithner, S., Klemm, C., Schlosser, A., Grossmann, A., Stelzl, U., Schraven, B., Krause, E., and Freund, C. (2010) Adhesion and degranulation promoting adapter protein (ADAP) is a central hub for phosphotyrosine-mediated interactions in T cells. *PloS one* **5,** e11708
19. Raab, M., Kang, H., da Silva, A., Zhu, X., and Rudd, C. E. (1999) FYN-T-FYB-SLP-76 interactions define a T-cell receptor zeta/CD3-mediated tyrosine phosphorylation pathway that up-regulates interleukin 2 transcription in T-cells. *J. Biol. Chem.* **274,** 21170–21179
20. Pauker, M. H., Reicher, B., Fried, S., Perl, O., and Barda-Saad, M. (2011) Functional cooperation between the proteins Nck and ADAP is fundamental for actin reorganization. *Mol. Cell. Biol.* **31,** 2653–2666
21. da Silva, A. J., Janssen, O., and Rudd, C. E. (1993) T cell receptor zeta/CD3-p59fyn(T)-associated p120/130 binds to the SH2 domain of p59fyn(T). *J. Exp. Med.* **178,** 2107–2113
22. Lange, S., Sylvester, M., Schumann, M., Freund, C., and Krause, E. (2010) Identification of phosphorylation-dependent interaction partners of the adapter protein ADAP using quantitative mass spectrometry: SILAC vs (18)O-labeling. *J. Proteome Res.* **9,** 4113–4122
23. Kuropka, B., Royla, N., Freund, C., and Krause, E. (2015) Sortase A mediated site-specific immobilization for identification of protein interactions in affinity purification-mass spectrometry experiments. *Proteomics* **15,** 1230–1234
24. Brill, L. M., Salomon, A. R., Ficarro, S. B., Mukherji, M., Stettler-Gill, M., and Peters, E. C. (2004) Robust phosphoproteomic profiling of tyrosine phosphorylation sites from human T cells using immobilized metal affinity chromatography and tandem mass spectrometry. *Anal. Chem.* **76,** 2763–2772
25. Cao, L., Ding, Y., Hung, N., Yu, K., Ritz, A., Raphael, B. J., and Salomon, A. R. (2012) Quantitative phosphoproteomics reveals SLP-76 dependent regulation of PAG and Src family kinases in T cells. *PLoS ONE* **7,** e46725
26. Ficarro, S. B., Salomon, A. R., Brill, L. M., Mason, D. E., Stettler-Gill, M., Brock, A., and Peters, E. C. (2005) Automated immobilized metal affinity chromatography/nano-liquid chromatography/electrospray ionization mass spectrometry platform for profiling protein phosphorylation sites. *Rapid Commun. Mass Spectrom.* **19,** 57–71
27. Kim, J. E., and White, F. M. (2006) Quantitative analysis of phosphotyrosine signaling networks triggered by CD3 and CD28 costimulation in Jurkat cells. *J. Immunol.* **176,** 2833–2843
28. Mayya, V., Lundgren, D. H., Hwang, S. I., Rezaul, K., Wu, L., Eng, J. K., Rodionov, V., and Han, D. K. (2009) Quantitative phosphoproteomic analysis of T cell receptor signaling reveals system-wide modulation of protein-protein interactions. *Sci. Signal.* **2,** ra46
29. Nguyen, V., Cao, L., Lin, J. T., Hung, N., Ritz, A., Yu, K., Jianu, R., Ulin, S. P., Raphael, B. J., Laidlaw, D. H., Brossay, L., and Salomon, A. R. (2009) A new approach for quantitative phosphoproteomic dissection of signaling pathways applied to T cell receptor activation. *Mol. Cell. Proteomics* **8,** 2418–2431
30. Ruperez, P., Gago-Martinez, A., Burlingame, A. L., and Oses-Prieto, J. A.

(2012) Quantitative phosphoproteomic analysis reveals a role for serine and threonine kinases in the cytoskeletal reorganization in early T cell receptor activation in human primary T cells. *Mol. Cell. Proteomics* **11,** 171–186
31. Ong, S. E., and Mann, M. (2006) A practical recipe for stable isotope labeling by amino acids in cell culture (SILAC). *Nat. Protoc.* **1,** 2650–2660
32. Cox, J., and Mann, M. (2008) MaxQuant enables high peptide identification rates, individualized p.p.b.-range mass accuracies and proteome-wide protein quantification. *Nat. Biotechnol.* **26,** 1367–1372
33. Boehm, M. E., Seidler, J., Hahn, B., and Lehmann, W. D. (2012) Site-specific degree of phosphorylation in proteins measured by liquid chromatography-electrospray mass spectrometry. *Proteomics* **12,** 2167–2178
34. Seidler, J., Adal, M., Kubler, D., Bossemeyer, D., and Lehmann, W. D. (2009) Analysis of autophosphorylation sites in the recombinant catalytic subunit alpha of cAMP-dependent kinase by nano-UPLC-ESI-MS/MS. *Anal. Bioanal. Chem.* **395,** 1713–1720
35. Vranken, W. F., Boucher, W., Stevens, T. J., Fogh, R. H., Pajon, A., Llinas, M., Ulrich, E. L., Markley, J. L., Ionides, J., and Laue, E. D. (2005) The CCPN data model for NMR spectroscopy: development of a software pipeline. *Proteins* **59,** 687–696
36. Zimmermann, J., and Freund, C. (2005) NMR assignment of the reduced and oxidized forms of the human ADAP hSH3–1 domain. *J. Biomol. NMR* **32,** 94
37. Folmer, R. H., Geschwindner, S., and Xue, Y. (2002) Crystal structure and NMR studies of the apo SH2 domains of ZAP-70: two bikes rather than a tandem. *Biochemistry* **41,** 14176–14184
38. Menasche, G., Kliche, S., Chen, E. J., Stradal, T. E., Schraven, B., and Koretzky, G. (2007) RIAM links the ADAP/SKAP-55 signaling module to Rap1, facilitating T-cell-receptor-mediated integrin activation. *Mol. Cell. Biol.* **27,** 4070–4081
39. Horn, J., Wang, X., Reichardt, P., Stradal, T. E., Warnecke, N., Simeoni, L., Gunzer, M., Yablonski, D., Schraven, B., and Kliche, S. (2009) Src homology 2-domain containing leukocyte-specific phosphoprotein of 76 kDa is mandatory for TCR-mediated inside-out signaling, but dispensable for CXCR4-mediated LFA-1 activation, adhesion, and migration of T cells. *J. Immunol.* **183,** 5756–5767
40. Hornbeck, P. V., Kornhauser, J. M., Tkachev, S., Zhang, B., Skrzypek, E., Murray, B., Latham, V., and Sullivan, M. (2012) PhosphoSitePlus: a comprehensive resource for investigating the structure and function of experimentally determined post-translational modifications in man and mouse. *Nucleic Acids Res.* **40,** D261–270
41. Chan, A. C., Iwashima, M., Turck, C. W., and Weiss, A. (1992) ZAP-70: a 70 kd protein-tyrosine kinase that associates with the TCR zeta chain. *Cell* **71,** 649–662
42. Zimmermann, J., Kuhne, R., Sylvester, M., and Freund, C. (2007) Redox-regulated conformational changes in an SH3 domain. *Biochemistry* **46,** 6971–6977
43. Piotukh, K., Kosslick, D., Zimmermann, J., Krause, E., and Freund, C. (2007) Reversible disulfide bond formation of intracellular proteins probed by NMR spectroscopy. *Free Radical Biol. Med.* **43,** 1263–1270
44. Luis, B. S., and Carpino, N. (2014) Insights into the suppressor of T-cell receptor (TCR) signaling-1 (Sts-1)-mediated regulation of TCR signaling through the use of novel substrate-trapping Sts-1 phosphatase variants. *FEBS J.* **281,** 696–707
45. Astoul, E., Edmunds, C., Cantrell, D. A., and Ward, S. G. (2001) PI 3-K and T-cell activation: limitations of T-leukemic cell lines as signaling models. *Trends Immunol.* **22,** 490–496
46. Duhr, S., and Braun, D. (2006) Why molecules move along a temperature gradient. *Proc. Natl. Acad. Sci. U.S.A.* **103,** 19678–19682
47. Majkut, P., Claussnitzer, I., Merk, H., Freund, C., Hackenberger, C. P., and Gerrits, M. (2013) Completion of proteomic data sets by Kd measurement using cell-free synthesis of site-specifically labeled proteins. *PloS One* **8,** e82352
48. Keppler, A., Gendreizig, S., Gronemeyer, T., Pick, H., Vogel, H., and Johnsson, K. (2003) A general method for the covalent labeling of fusion proteins with small molecules in vivo. *Nat. Biotechnol.* **21,** 86–89
49. Roncagalli, R., Hauri, S., Fiore, F., Liang, Y., Chen, Z., Sansoni, A., Kanduri, K., Joly, R., Malzac, A., Lahdesmaki, H., Lahesmaa, R., Yamasaki, S., Saito, T., Malissen, M., Aebersold, R., Gstaiger, M., and Malissen, B. (2014) Quantitative proteomics analysis of signalosome dynamics in primary T cells identifies the surface receptor CD6 as a Lat adaptor-independent TCR signaling hub. *Nat. Immunol.* **15,** 384–392
50. Evans, R., Lellouch, A. C., Svensson, L., McDowall, A., and Hogg, N. (2011) The integrin LFA-1 signals through ZAP-70 to regulate expression of high-affinity LFA-1 on T lymphocytes. *Blood* **117,** 3331–3342
51. Kliche, S., Worbs, T., Wang, X., Degen, J., Patzak, I., Meineke, B., Togni, M., Moser, M., Reinhold, A., Kiefer, F., Freund, C., Forster, R., and Schraven, B. (2012) CCR7-mediated LFA-1 functions in T cells are regulated by 2 independent ADAP/SKAP55 modules. *Blood* **119,** 777–785
52. Lin, Y. P., Cheng, Y. J., Huang, J. Y., Lin, H. C., and Yang, B. C. (2010) Zap70 controls the interaction of talin with integrin to regulate the chemotactic directionality of T-cell migration. *Mol. Immunol.* **47,** 2022–2029
53. Coussens, N. P., Hayashi, R., Brown, P. H., Balagopalan, L., Balbo, A., Akpan, I., Houtman, J. C., Barr, V. A., Schuck, P., Appella, E., and Samelson, L. E. (2013) Multipoint binding of the SLP-76 SH2 domain to ADAP is critical for oligomerization of SLP-76 signaling complexes in stimulated T cells. *Mol. Cell. Biol.* **33,** 4140–4151
54. Hatada, M. H., Lu, X., Laird, E. R., Green, J., Morgenstern, J. P., Lou, M., Marr, C. S., Phillips, T. B., Ram, M. K., Theriault, K., and et al. (1995) Molecular basis for interaction of the protein tyrosine kinase ZAP-70 with the T-cell receptor. *Nature* **377,** 32–38
55. O'Brien, R., Rugman, P., Renzoni, D., Layton, M., Handa, R., Hilyard, K., Waterfield, M. D., Driscoll, P. C., and Ladbury, J. E. (2000) Alternative modes of binding of proteins with tandem SH2 domains. *Protein Sci* **9,** 570–579
56. Stephanowitz, H., Lange, S., Lang, D., Freund, C., and Krause, E. (2012) Improved two-dimensional reversed phase-reversed phase LC-MS/MS approach for identification of peptide-protein interactions. *J. Proteome Res.* **11,** 1175–1183
57. Kumar, A., Humphreys, T. D., Kremer, K. N., Bramati, P. S., Bradfield, L., Edgar, C. E., and Hedin, K. E. (2006) CXCR4 physically associates with the T cell receptor to signal in T cells. *Immunity* **25,** 213–224
58. Jackson, S. H., Devadas, S., Kwon, J., Pinto, L. A., and Williams, M. S. (2004) T cells express a phagocyte-type NADPH oxidase that is activated after T cell receptor stimulation. *Nat. Immunol.* **5,** 818–827
59. Witte, A., Degen, J., Baumgart, K., Waldt, N., Kuropka, B., Freund, C., Schraven, B., and Kliche, S. (2012) Emerging Roles of ADAP, SKAP55, and SKAP-HOM for Integrin and NF-κB Signaling in T cells. *J. Clin. Cell. Immunol.* doi:10.4172/2155–9899.S12–002
60. Koretzky, G. A., Abtahian, F., and Silverman, M. A. (2006) SLP76 and SLP65: complex regulation of signalling in lymphocytes and beyond. *Nat. Rev. Immunol.* **6,** 67–78
61. Wang, H., and Rudd, C. E. (2008) SKAP-55, SKAP-55-related and ADAP adaptors modulate integrin-mediated immune-cell adhesion. *Trends Cell Biol.* **18,** 486–493
62. Garcia-Bernal, D., Parmo-Cabanas, M., Dios-Esponera, A., Samaniego, R., Hernan, P. d. l. O. D., and Teixido, J. (2009) Chemokine-induced Zap70 kinase-mediated dissociation of the Vav1-talin complex activates alpha4beta1 integrin for T cell adhesion. *Immunity* **31,** 953–964